Human Molecular Genetics, 2019, Vol. 28, No. 15 2561–2572

doi: 10.1093/hmg/ddz079
Advance Access Publication Date: 22 April 2019
General Article

GENERAL ARTICLE

Targeted knock-in mice with a human mutation in GRTH/DDX25 reveals the essential role of phosphorylated GRTH in spermatid development during spermatogenesis

Raghuveer Kavarthapu[1], Rajakumar Anbazhagan[1], Murugananthkumar Raju[1], Chon-Hwa Tsai Morris[1], James Pickel[2] and Maria L. Dufau[1,*]

[1]Section on Molecular Endocrinology, Division of Developmental Biology, *Eunice Kennedy Shriver* National Institute of Child Health and Human Development, National Institutes of Health, Bethesda, MD 20892, USA and [2]Transgenic Core, National Institute of Mental Health, National Institutes of Health, Bethesda, MD 20892, USA

*To whom correspondence should be addressed at: Section on Molecular Endocrinology, NICHD, National Institutes of Health, Bethesda, MD 20892, USA. Tel: 301-496-2021; Email: dufaum@mail.nih.gov

Abstract

Gonadotropin-regulated testicular RNA helicase (GRTH/DDX25) is a testis specific member of the DEAD-box family of RNA helicases expressed in meiotic and haploid germ cells which plays an essential role in spermatogenesis. There are two species of GRTH the 56 kDa non-phospho and 61 kDa phospho forms. Our early studies revealed a missense mutation ($R^{242}H$) of GRTH in azoospermic men that when expressed in COS1-cells lack the phospho-form of GRTH. To investigate the role of the phospho-GRTH species in spermatogenesis, we generated a GRTH knock-in (KI) transgenic mice with the $R^{242}H$ mutation. GRTH-KI mice are sterile with reduced testis size, lack sperm with spermatogenic arrest at round spermatid stage and loss of the cytoplasmic phospho-GRTH species. Electron microscopy studies revealed reduction in the size of chromatoid bodies (CB) of round spermatids (RS) and germ cell apoptosis. We observed absence of phospho-GRTH in the CB of RS. Complete loss of chromatin remodeling and related proteins such as TP2, PRM2, TSSK6 and marked reduction of their respective mRNAs and half-lives were observed in GRTH-KI mice. We showed that phospho-GRTH has a role in TP2 translation and revealed its occurrence in a 3′ UTR dependent manner. These findings demonstrate the relevance of phospho-GRTH in the structure of the chromatoid body, spermatid development and completion of spermatogenesis and provide an avenue for the development of a male contraceptive.

Introduction

Gonadotropin-regulated testicular RNA helicase (GRTH/Ddx25), a member of the DEAD-box protein family of RNA helicase, is hormonally regulated by gonadotropins. GRTH is a testis specific protein expressed in Leydig cells and germ cells (predominantly in meiotic spermatocytes (SP) and haploid spermatids) (1–4). It is a post-transcriptional regulator of genes which are essential

Received: January 4, 2019. **Revised:** March 15, 2019. **Accepted:** March 21, 2019

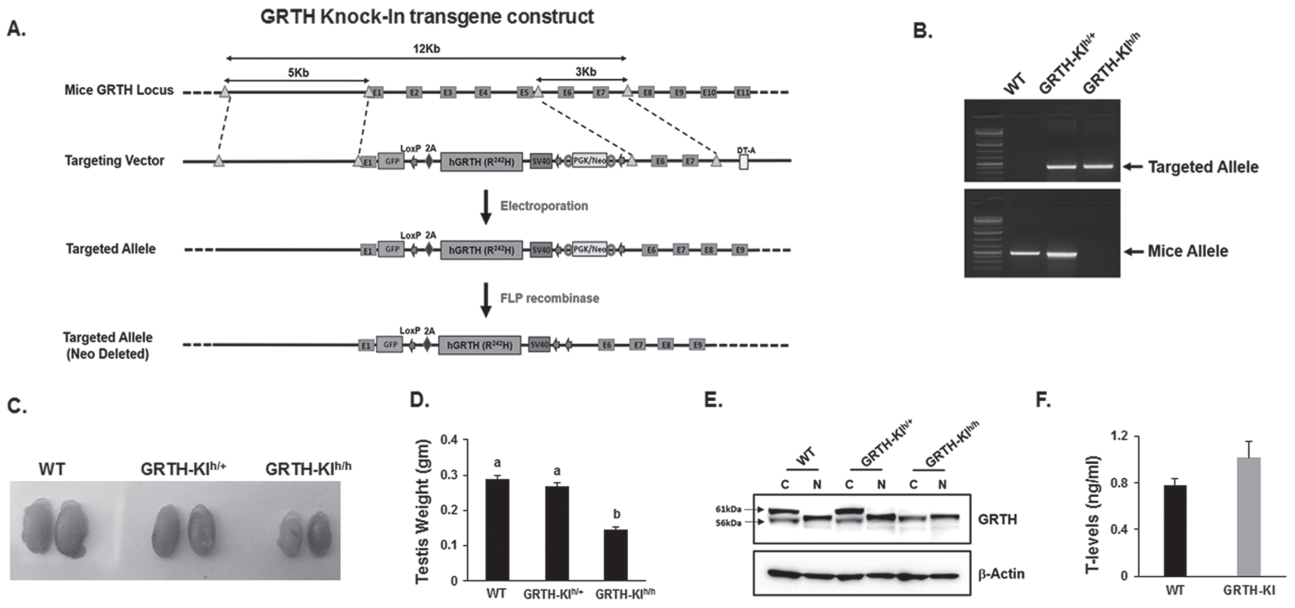

Figure 1. Strategy for production of GRTH-KI mice. (**A**) Generation of the GRTH-KI mice. Targeting vector containing GRTH cDNA with $R^{242}H$ mutation, PGK-Neo cassette flanked by FRT sites as described in materials and methods section was used to replace exons 1–5 of mouse GRTH. Chimeric animals were bred and subsequently crossed with a mice expressing Flp recombinase to remove the PGK-Neo cassatte. (**B**) Genotyping by PCR for determination of WT, GRTH-$KI^{h/+}$ (heterozygous) and GRTH-$KI^{h/h}$ (homozygous) mice. (**C**) Image showing size of the mice testes. Testes from homozygous KI mice are smaller compared with those from wild-type and heterozygote KI mice. (**D**) Mean testis weight for WT, GRTH-$KI^{h/+}$ and GRTH-$KI^{h/h}$ mice ($n = 8$). Different superscript letters indicate significant differences (Tukey's multiple comparison test, $P < 0.05$). (**E**) Western blot showing the expression of phospho-GRTH and non phospho-GRTH in testis of WT, GRTH-$KI^{h/+}$ and GRTH-$KI^{h/h}$ mice. (**F**) Serum testosterone levels of WT and GRTH-$KI^{h/h}$ mice ($n = 6$). Statistical analysis were performed using Student's *t*-test (* indicates $P < 0.001$) and data represents mean ± SEM.

for completion of spermatogenesis. As an integral component of ribonuclear particles, GRTH functions as a shuttling protein that transport specific mRNAs from the nucleus to cytoplasmic sites of germ cells via the chromosomal maintenance 1 pathway. In the cytoplasm of round spermatids (RS), the RNA of specific germ cell genes are likely stored in chromatoid bodies (CB) in association with GRTH prior to their translation at specific times during spermatogenesis (3,5). GRTH associates with actively translating polyribosomes and believed to regulate translation of specific germ cell genes and the expression of key proteins that participate in sperm maturation including transition proteins (TP1 and TP2), phosphoglycerate kinase (PGK2), testicular angiotensin converting enzyme (tACE) and protamines (PRM) 1 and 2 (6,7). GRTH null mice are sterile, lack elongated spermatids (ES) and spermatozoa due to failure of RS to elongate, resulting from complete arrest at step 8 of spermiogenesis. There is marked reduction in size of the CB in RS of GRTH null mice which is consistent with either absence or decrease of nuclear-cytoplasmic transport of messages relevant to spermiogenesis (5,7). GRTH is the only member of the DEAD-box helicase family known to be transcriptionally up-regulated by a hormone. In Leydig cells, luteinizing hormone/via its receptor through stimulation of androgen production supports GRTH transcription in an autocrine fashion through an androgen responsive element present in proximal region of the GRTH gene (8). In germ cells, where GRTH expression is both cell- and stage-specific, paracrine actions of androgen via its receptors in Sertoli cells increase transcription of GRTH in germ cells. Androgen through an unknown mechanism increases germ cell nuclear factor in germ cells which in turn binds its element at a distal region of the GRTH gene and specifically regulates its expression in RS (9–11). In Leydig cells, GRTH regulates the expression of genes involved in cholesterol synthesis (SREBP2, HMG-CoA) and its transport (StAR) to the inner mitochondrial membrane and exerts a negative autocrine control of androgen production (12).

The GRTH gene is TATA-less with multiple transcriptional start sites and its transcriptional activity is driven by Sp1/Sp3 (13). In germ cells, there are two GRTH protein species, a 61 kDa phosphorylated form and a 56 kDa non-phosphorylated form. The 61 kDa phospho-GRTH resides exclusively at cytoplasmic sites is believed to shuttle messages to and from the CB and to polyribosomes for translation. The 56 kDa non-phospho form transports relevant messages from the nucleus to the cytoplasm (3,6).

Previous studies from our laboratory identified polymorphic forms of *GRTH* by screening infertile Japanese men with non-obstructive azoospermia. A missense heterozygous mutation found in exons 8 resulted in a single amino acid change, Arg 242 to His ($R^{242}H$) (14). *In vitro* experiments overexpressing this mutant form in COS-1 cells revealed that the mutation of $R^{242}H$ in the GRTH gene abolished the phosphorylation of GRTH and as result the 61 kDa phospho protein was not found in the cytoplasm, while the expression of the nuclear non-phospho 56 kDa species was preserved (14). We have also shown that protein kinase A is responsible for the phosphorylation of GRTH protein (6). The above findings provided an avenue to differentially explore the functional role of phospho-form from the non-phospho GRTH species. Towards this goal, we generated a GRTH knock-in (KI) transgenic mice carrying the GRTH gene with the $R^{242}H$ mutation and demonstrated the essential role of phospho-GRTH species in the progress of spermatogenesis.

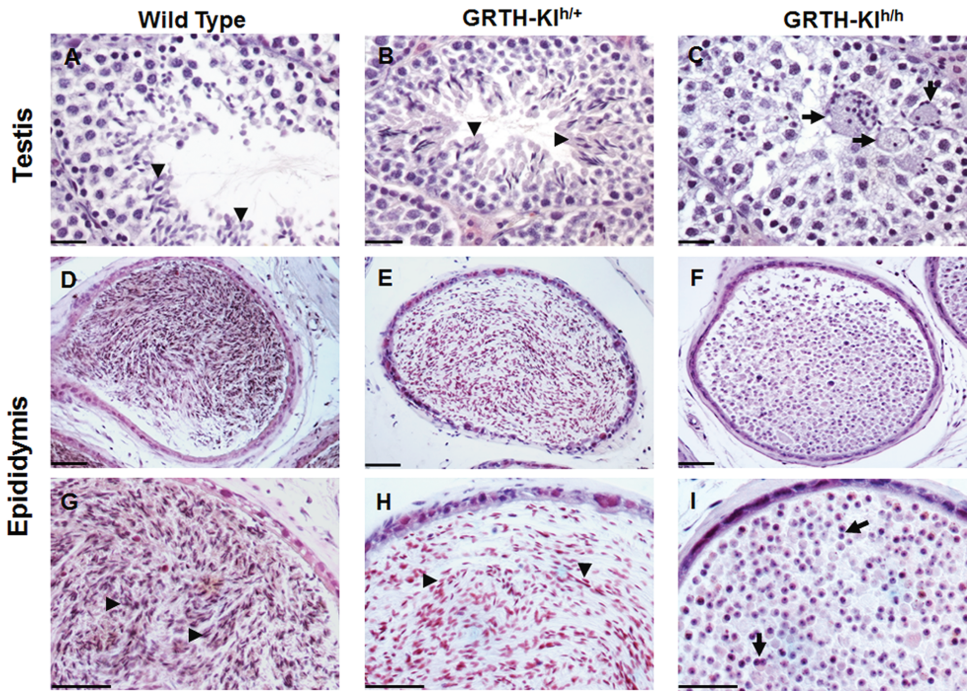

Figure 2. Morphological defects in the GRTH-KI$^{h/h}$ mice testis (**A**), (**B**) and (**C**) H&E staining of WT, GRTH-KI$^{h/+}$ and GRTH-KI$^{h/h}$ testis, respectively showing seminiferous tubules. Arrowheads, indicate presence of ES only in WT and GRTH-KI$^{h/+}$ mice tesis. Arrows, indicate degenerating multinucleated giant cells in GRTH-KI$^{h/h}$ mice. (**D**), (**E**) and (**F**) H&E staining of epididymis showing lumens occupied with mature sperm in WT and GRTH-KI$^{h/+}$ mice while GRTH-KI$^{h/h}$ mice are devoid of sperm. (**G**), (**H**) and (**I**) Higher magnification of epididymis showing lumens filled with mature sperm (arrowheads) in WT and GRTH-KI$^{h/+}$ mice while GRTH-KI$^{h/h}$ mice lumens contain degenerating/apoptotic RS (arrows). Scale bar is 50 µm.

Results

Generation of GRTH-KI Transgenic mice

In order to investigate the essential role of phospho-GRTH species in spermatogenesis, we generated a GRTH-KI transgenic mice carrying the human GRTH gene with the $R^{242}H$ mutation that was found in Japanese infertile men. The GRTH-KI transgenic mouse was achieved by knocking out/removing exons 1–5 of the mice GRTH and replacing these with the targeting vector which contain the human GRTH cDNA with the $R^{242}H$ mutation and a PGK-Neo cassette (Fig. 1A). We used the Flp-FRT system to obtain GRTH-KI mice with the PGK-Neo cassette removed by crossing the chimeras with *FLP* deleter mice (Fig. 1A). The offprings were genotyped using two specific primer sets one for targeted allele and other for mice allele to determine homozygous (GRTH-KI$^{h/h}$) and heterozygous (GRTH-KI$^{h/+}$) transgenic mice lines (Fig. 1B). We also confirmed the $R^{242}H$ mutation in GRTH-KI mice by sequencing the exon 8 region of GRTH gene. The breeding experiments of GRTH-KI$^{h/h}$ and GRTH-KI$^{h/+}$ male with wild-type (WT) female mice revealed that GRTH-KI$^{h/h}$ are sterile while the GRTH-KI$^{h/+}$ are fertile and gave rise to offsprings. Further, we observed reduction in testicular size (Fig. 1C) and weight (Fig. 1D) in GRTH-KI$^{h/h}$ mice when compared to WT and GRTH-KI$^{h/+}$ male mice. Western blot was performed to evaluate the expression of GRTH in cytosolic and nuclear fractions obtained from testes of WT and GRTH-KI mice. We found complete loss of the 61 kDa phospho-GRTH species in the germ cell cytosolic fraction of GRTH-KI$^{h/h}$ mice when compared to WT and GRTH-KI$^{h/+}$ mice (Fig. 1E). Serum testosterone levels in GRTH-KI$^{h/h}$ were not different from WT mice (Fig. 1F). This indicates that the mutation resulting in loss of phospho-GRTH in GRTH-KI$^{h/h}$ mice does not affect basal androgen production and as result the mating behavior in these mice was normal.

Role of phospho-GRTH in spermatogenesis

Histological examination of seminiferous tubules of GRTH-KI$^{h/h}$ mice (Fig. 2C) testis revealed lack of ES compared to WT mice (Fig. 2A). The GRTH-KI$^{h/+}$ mice testis showed normal signs of germ cell development with progression of RS into ES and spermatozoa (Fig. 2B). GRTH-KI$^{h/h}$ mice displayed sloughing of pachytene SP and degenerating multinucleated giant cells, indicative of early apoptosis (Fig. 2C). The epididymis of GRTH-KI$^{h/h}$ mice is devoid of mature sperm and is filled with degenerating/apoptotic spermatids while WT and GRTH-KI$^{h/+}$ mice epididymis contain mature sperm (Fig. 2D–I). Further analysis using periodic acid/Schiff (PAS) staining in GRTH-KI$^{h/h}$ mice testis revealed global arrest of spermatogenesis at round spermatid stage. The RS fail to elongate at step 8 of spermiogenesis. WT spermatids at stage VIII (step 7–8 of spermatogenesis) had arc-shaped acrosome with distintive PAS-positive acrosomal cap, while GRTH-KI$^{h/h}$ had RS showing a range of abnormalities in acrosomes with asymmetric formation and displacement of the acrosomal granule (Fig. 3A). Typically WT seminiferous tubules in stage XII of spermatogenesis contain meiotic SP, ES and no RS while GRTH-KI$^{h/h}$ testis had meiotic SP and RS that fail to elongate, thus lacking ES. EM analysis of RS in GRTH-KI$^{h/h}$ mice also showed irregular shaped acrosomes lacking the distinct acrosomal cap-like structure found in WT mice (Fig. 3B).

Loss of GRTH in CB in GRTH-KI$^{h/h}$ mice

EM studies of GRTH-KI$^{h/h}$ mice testis revealed either complete loss or a significant reduction in the size of CB residing in the cytoplasm of RS in the vicinity of the nucleus compared to WT mice where in the CB have typical amorphous 'nuage' texture

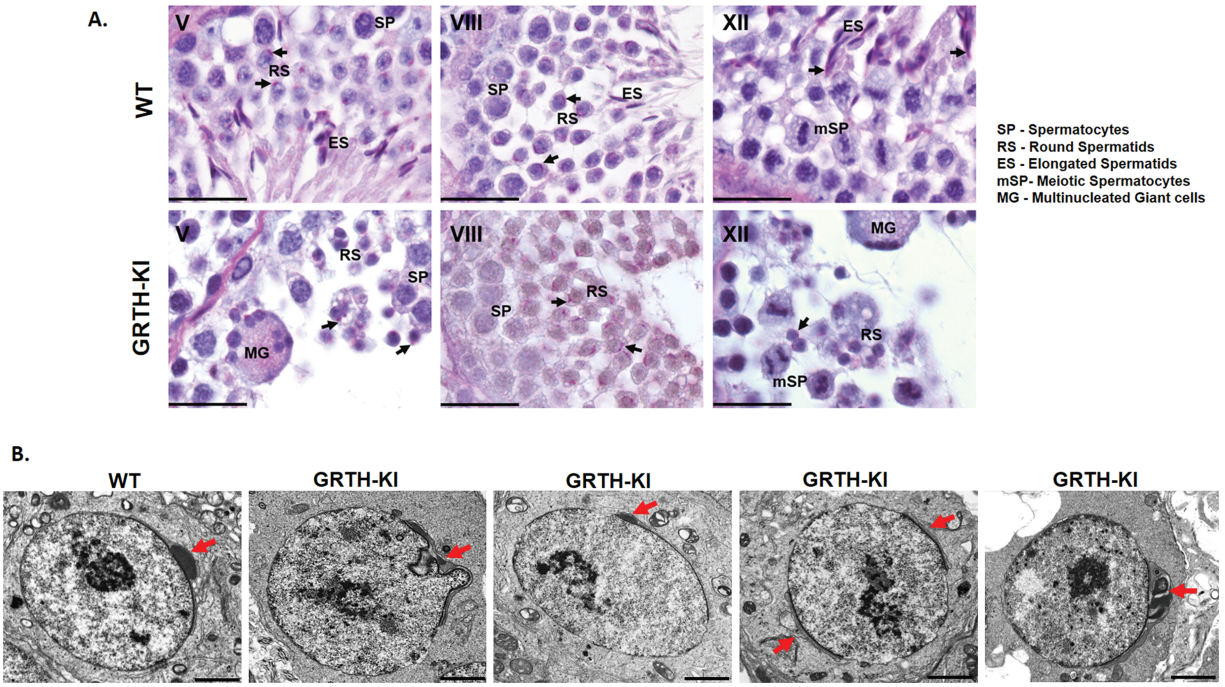

Figure 3. Spermatogenic arrest in GRTH-KI$^{h/h}$ mice (**A**) PAS staining showing acrosome structures (arrows) in WT and GRTH-KI$^{h/h}$ testis sections. Presence of RS with acrosomal staining in stage XII of spermatogenesis in GRTH-KI$^{h/h}$ mice indicating complete spermatogenic arrest at round spermatid stage where RS fail to elongate at step 8 of spermiogenesis. (**B**) EM sections of RS showing abnormalities in acrosomes (red arrows) in GRTH-KI$^{h/h}$ mice compared to normal distinct cap-shaped acrosome in WT mice. Scale bar is 50 µm.

(Fig. 4A). Immunofluorescence studies showed the presence of GRTH in the nucleus and in the CB which resides in cytoplasm of RS in WT mice. However, in GRTH-KI$^{h/h}$ mice there was complete loss of expression of GRTH in CB, while the non-phospho form is present in the nucleus and also scattered in the cytoplasm (Fig. 4B). From these studies we deduce that phospho-GRTH is present in the CB in addition to its distribution at other cytoplasmic sites (i.e. polyribosomes; 15).

Phospho form of GRTH prevents testicular germ cell apoptosis

EM analysis of seminiferous tubules in GRTH-KI$^{h/h}$ mice showed degenerating germ cells with signs of apoptosis that include nuclear membrane disintegration, chromatin condensation and break-down, and formation of abundant vacuoles in the cytoplasm compared to germ cells of WT mice (Fig. 5A). The development of RS ceased at step 8, and no progression to elongating spermatids (indicated by black arrows in WT mice) was observed in GRTH-KI$^{h/h}$ mice (Fig. 5A). TUNEL assay was performed to examine whether loss of phospho-GRTH form causes germ cells apoptosis. A significant increase in apoptotic germ cells was observed in KI mice compared to WT mice (Fig. 5B). We also observed an increase in expression of pro-apoptotic protein BH3 interacting-domain death agonist and a decrease in anti-apoptotic protein B-cell lymphoma 2 in GRTH-KI$^{h/h}$ mice compared to WT mice (Fig. 5C). In addition, it is noted that significant increase in cleaved products of caspase 9 and poly ADP ribose polymerase in GRTH-KI$^{h/h}$ mice compared to WT mice (Fig. 5C). These findings clearly show that lack of phospho-GRTH results in degeneration/apoptosis of RS that failed to develop and elongate. Although considerable apoptosis was also observed in pachytene SP in GRTH-KI$^{h/h}$ mice, germ cells continue to progress to step 8 of RS.

Phospho-GRTH regulates expression of chromatin remodeling genes Tp2 and Prm2

We evaluated total and cytoplasmic mRNA and protein levels of TP2, PRM2, tACE and high mobility group box 2 (HMG2), testis-specific serine/threonine-protein kinase 6 (TSSK6) and GRTH by real-time PCR (Fig. 6A and B) and western blotting (Fig. 6C), in WT and GRTH-KI$^{h/h}$ mice testis. In KI mice, we observed significant reduction in total and cytoplasmic mRNA levels and complete loss of TP2, PRM2 and TSSK6 proteins compared to WT mice (Fig. 6A–C). In contrast, mRNA and protein levels of HMG2 and tACE were unchanged. GRTH total mRNA levels were not different from controls while cytoplasmic levels were reduced. As expected the 61 kDa phospho-protein form of GRTH was not present. GRTH is known to associate/bind with mRNA of chromatin remodeling genes *Tp2* and *Prm2* and participate in their export in the nucleus (7). In GRTH-KI$^{h/h}$ mice, we observed no change or increase in the association/binding of GRTH protein with *Tp2* and *Prm2* mRNAs in the nuclear extracts compared to WT (Fig. 7A and B). However, in cytosolic extracts of GRTH-KI$^{h/h}$ mice there was low to negligible levels of association of GRTH protein with *Tp2* and *Prm2* mRNAs compared to WT mice (Fig. 7D and E). *Tp2* and *Prm2* messages either degraded or not translated as a result of lack of the phospho-GRTH and this led to absence of these proteins (TP2 and PRM2) in GRTH-KI$^{h/h}$ mice testis as shown by western blotting (Fig. 6A). These results indicate that phospho-GRTH associates with *Tp2* and *Prm2* mRNA in cytoplasm and control their expression by presumably regulating either cytoplasmic transport of selective mRNA mes-

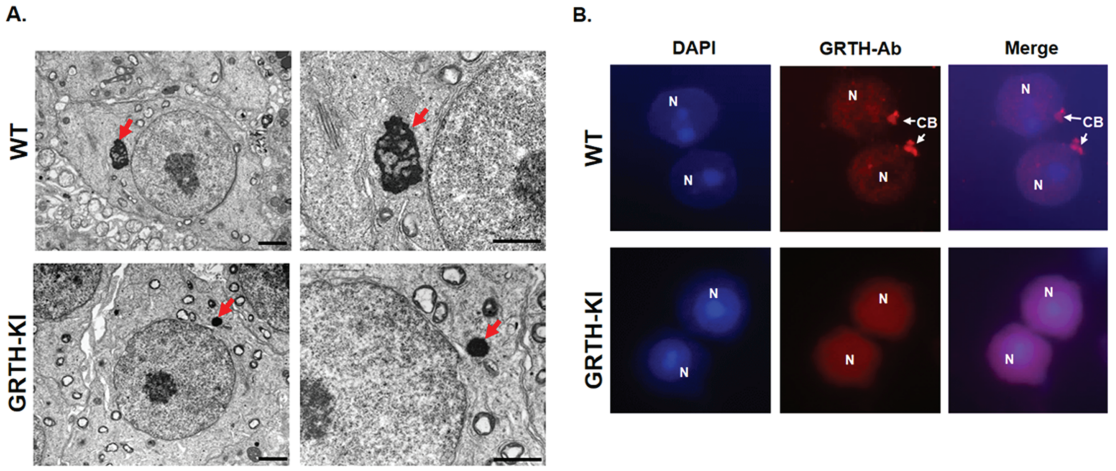

Figure 4. Morphological changes and loss of GRTH in CB in RS of GRTH-KI$^{h/h}$ mice. (**A**) EM sections of RS showing marked size reduction in chromatoid body (red arrows) in GRTH-KI$^{h/h}$ mice compared to WT mice. (**B**) Immunofluoresence staining shows expression of GRTH protein in the nucleus and at cytoplasmic sites, in CBs of RS of WT mice. Arrows indicate CB. GRTH-KI$^{h/h}$ mice lack GRTH signal in the CB, but show dispersed scarce GRTH signals at cytoplasmic sites and its presence in the nucleus is comparable to the WT. Nucleus is indicated as N. Scale bar is 1 μm.

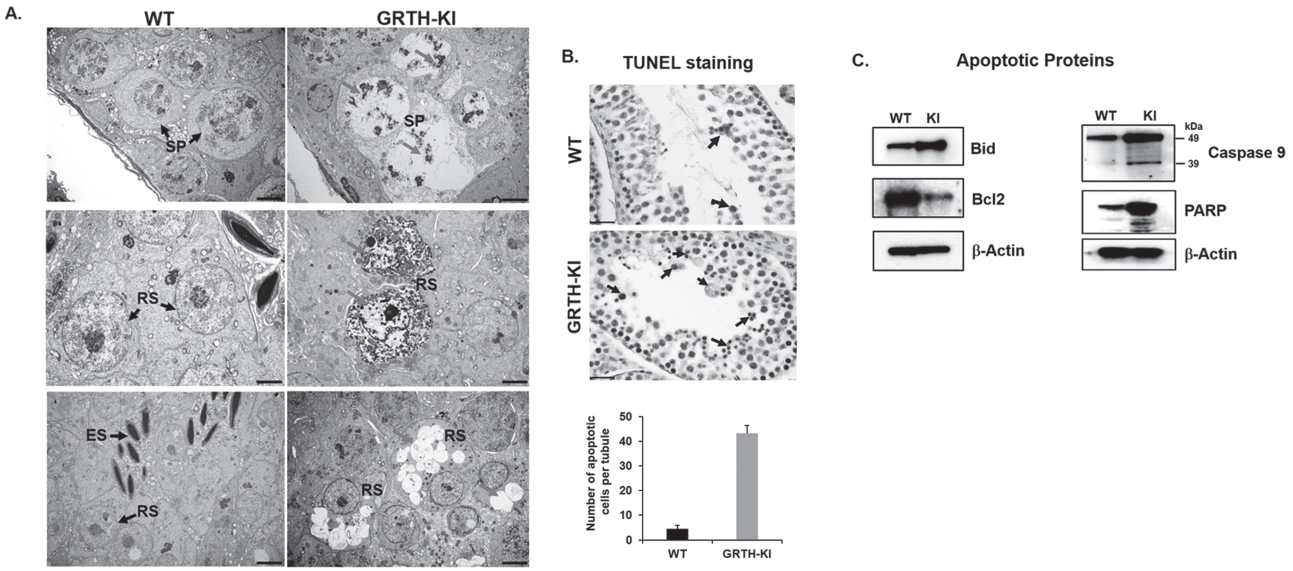

Figure 5. Testicular germ cell apoptosis in GRTH-KI$^{h/h}$ mice. (**A**) EM sections showing normal healthy SP and RS in WT mice while GRTH-KI$^{h/h}$ mice testis show sloughing of pachytene SP from the seminiferous epithelium and apoptotic SP and RS with disintegrating chromatin, loss of nuclear membrane and large vacuoles in the cytoplasm. Spermatocytes (SP), round spermatids (RS), elongated spermatids (ES). Scale bar is 1 μm. (**B**) TUNEL IHC staining (above) of testis section from GRTH-KI$^{h/h}$ mice show marked apoptosis in RS and multinucleate cysts compared to WT mice. Scale bar is 50 μm. Quantitative evaluation of apoptosis (bottom), mean ± SE of apoptotic cells per tubule (10 tubules were assessed for each group. (**C**) Western blots of pro- and anti- apoptotic proteins in WT versus GRTH-KI mice.

sages and/or their translation process of these proteins during spermiogenesis. We observed a significant reduction in the association of GRTH protein with its own mRNA in the cytosolic extracts of GRTH-KI$^{h/h}$ mice testis compared to WT (Fig. 7F), while a significantly increased association was found in the nuclear extracts of GRTH-KI$^{h/h}$ mice testis compared to WT (Fig. 7C). The reduced levels of total mRNA of *Tp2*, *Prm2* and *Tssk6* observed (Fig. 6A) in GRTH-KI$^{h/h}$ mice are related to marked reduction in cytosolic mRNA (Fig. 6B) and arrest at stage 8 of RS. This is particularly relevant to TSSK6 whose mRNAs are present in RS but translation is effected in ES while TP2 mRNA and protein are present in RS (16). The major reduction in the cytoplasm of GRTH mRNA in GRTH-KI$^{h/h}$ mice compared with WT mice relates to the absence of phospho-GRTH which is exclusively found in the cytoplasm of germ cells (Fig. 6B). Taken into account that the relative binding of GRTH is increased in the nuclear compartment for TP2, PRM2, their reduced protein expression likely result from lack of phospho-GRTH at cytoplasmic sites.

miRNA expression of miR469, miR34c and Let7e

Our previous work on GRTH knock-out (KO) mice demonstrated a role of GRTH as negative regulator of miRNA biogenesis. A subset of microRNAs were found to be upregulated in RS of GRTH-KO mice including testis specific miR469, testis preferred miR34c and miR470 and ubiquitous let-7 family members, and others (17). Since miRNA 469, which is markedly increased in GRTH-KO, was demonstrated to repress TP2 and PRM2 protein expression and to have only minor effects in mRNA degradation it was of interest to learn whether phospho-GRTH participated in the regulation of these relevants miRNAs. Real time RT-PCR analysis of selective testis specific miRNAs (miR469, miR34c),

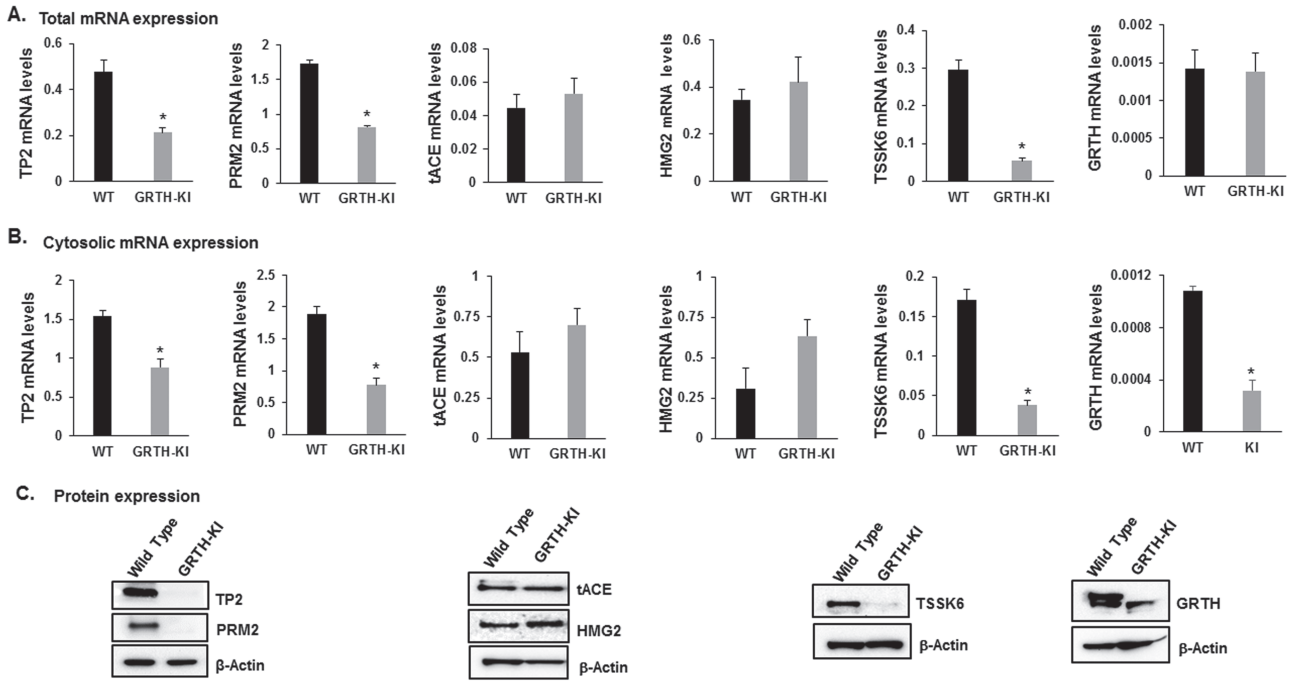

Figure 6. Protein and mRNA expression of chromatin remodeling genes TP2 and PRM2, TSSK6, tACE, HMG2 and GRTH in WT and GRTH-KI$^{h/h}$ mice. (**A**) Evaluation of total mRNA and (**B**) cytosolic mRNA levels in WT and GRTH-KI$^{h/h}$ mice. (**C**) Western blots showing protein expression in WT mice and GRTH-KI$^{h/h}$ mice.

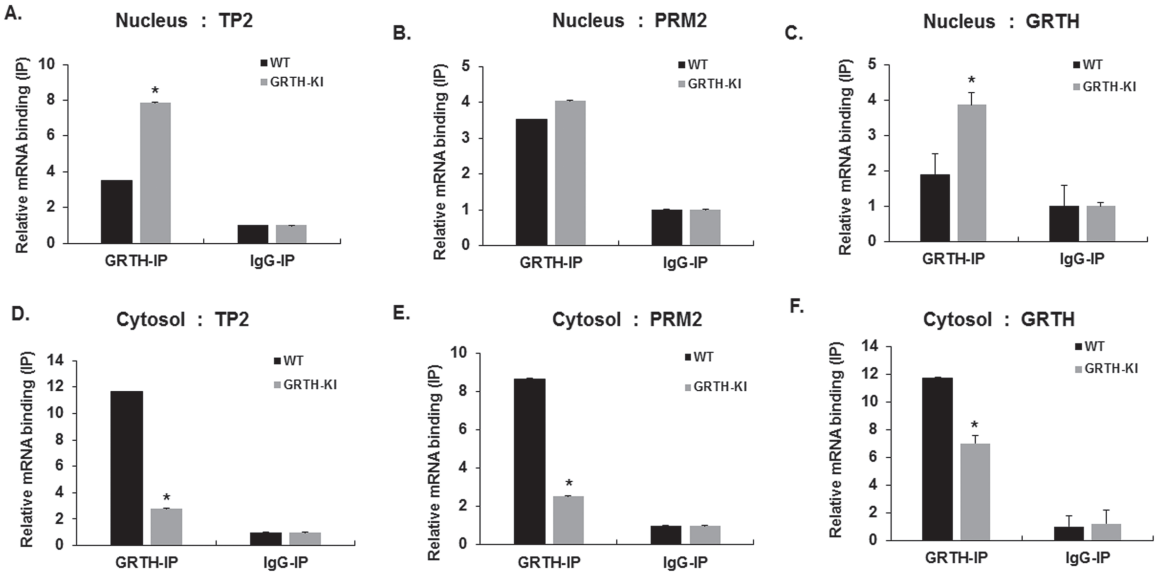

Figure 7. Binding of GRTH to specific germ cells mRNAs, (TP2 and PRM2) and its own message in WT and GRTH-KI$^{h/h}$ mice. Relative *Tp2* mRNA (**A**), *Prm2* mRNA (**B**) and *GRTH* mRNA (**C**) binding to GRTH protein in cytosolic and nuclear extracts of testis from WT and KI mice. All statistical analysis were performed using Student's *t*-test (* indicates $P < 0.05$) and data represents mean ± SEM of two independent experiments in triplicates.

and Let7e showed no significant change in their levels in WT and GRTH-KI$^{h/h}$ mice (Fig. 8A) indicating that phospho-GRTH was not involved in the regulation of relevant miRNAs affected in KO mice.

GRTH stimulates TP2 translation in a 3′ UTR dependent manner

Previously, we have shown that GRTH protein binds to 3′(untranslated region)UTR of *Tp2* mRNA (18). To learn whether GRTH has a role in the stimulation of *Tp2* mRNA translation, we performed luciferase assay in COS-1 cells co-transfected with psi-CHECK2 construct containing the *Tp2* coding region with its 3′ UTR and a GRTH expression construct. In addition, GRTH phosphorylation was induced by overexpressing the PKA catalytic subunit in COS-1 cells. We observed a dramatic increase in the renilla activity in samples expressing both GRTH and PKA (Fig 8B). In contrast, this increase in renilla luciferase activity was abolished when a mutant form of GRTH ($R^{242}H$) protein was expressed in presence or absence of PKA in COS-1 cells (Fig. 8B).

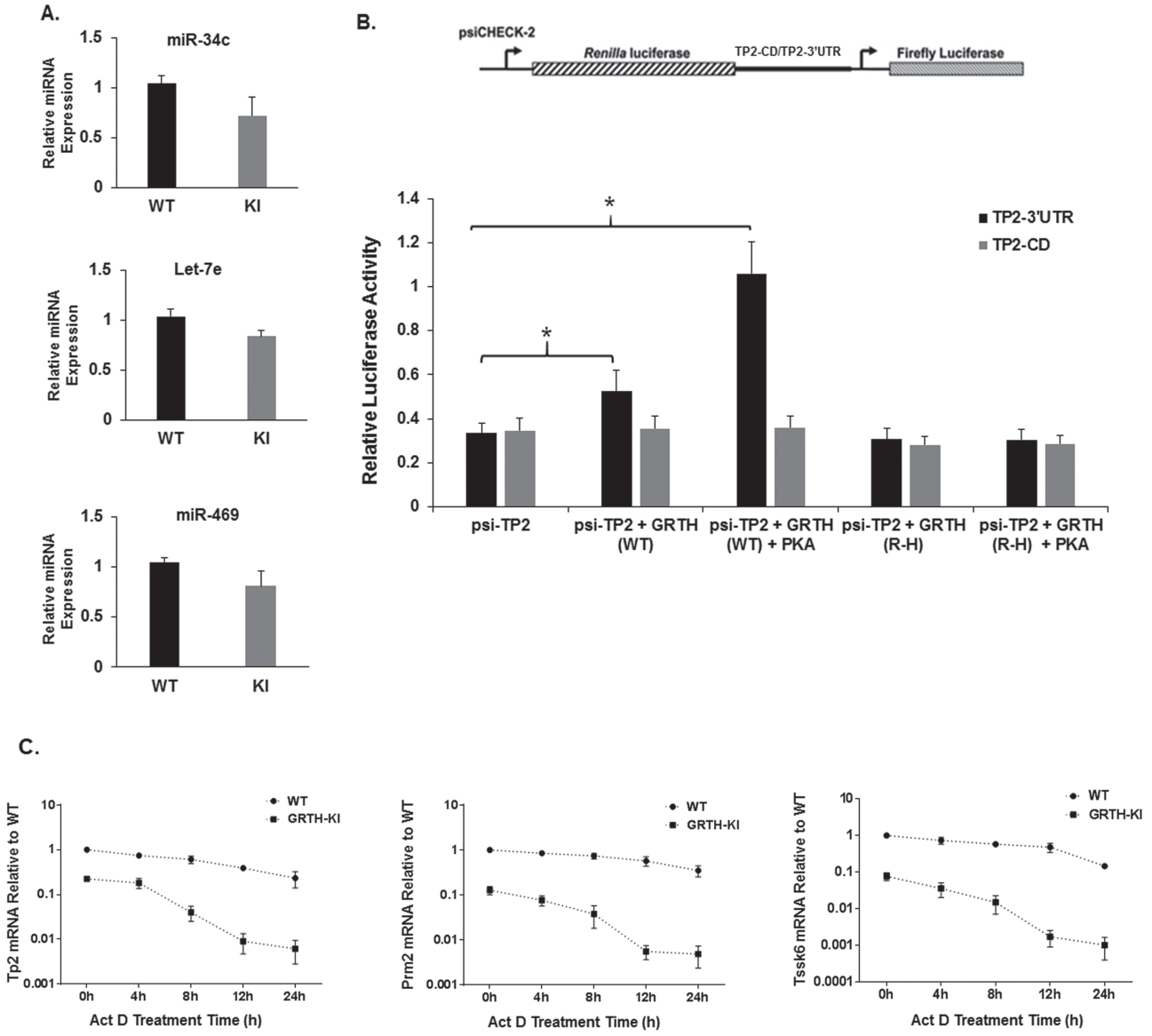

Figure 8. Role of phospho-GRTH on testis-specific miRNAs regulation, mRNA stability and translation in a 3′ UTR dependent manner. (**A**) Expression levels of testis-specific miRNA (miR469, miR34C) and Let7e in WT and GRTH-KI$^{h/h}$ mice. (**B**) Stimulation of translation of TP2 by GRTH depends on the presence of TP2 3′ UTR region. Schematic representation of the psiCheck2 reporter gene carrying the TP2 coding sequence with or without 3′ UTR (Above). Relative Luciferase activity in COS-1 cells co-transfected with these reporter TP2 constructs and GRTH (WT) or with GRTH (R-H mutant) expression constructs, and with or without PKA catalytic alpha subunit expression construct or empty vector (Below). TP2–3′UTR (TP2 coding region with 3′ UTR), TP2-CD (TP2 coding region only without 3′ UTR). Asterisks (*) indicate statistically significant change between psi-TP2 and psi-TP2 + GRTH + PKA groups (Student's *t*-test; $P < 0.05$). All the data for Figure 8 represent mean ± SE of three independent experiments. (**C**) mRNA stability assay showing relative levels of *Tp2*, *Prm2* and *Tssk6* mRNAs from WT and GRTH-KI$^{h/h}$ seminiferous tubule cultures treated with Actinomycin-D (20 ng/ml) at different time points (0 h, 4 h, 8 h, 12 h and 24 h).

Also, lack of stimulation was observed when the 3′UTR was not present indicating its relevance on TP2 translation.

Lack of phospho-GRTH leads to *Tp2*, *Prm2* and *Tssk6* mRNA degradation

To investigate the role of phospho-GRTH in the mRNA stability of *Tp2*, *Prm2* and *Tssk6*, we measured the mRNA half-lives of these genes by analyzing the expression levels of mRNA at different time points after treatment with Actinomycin-D. The half-lives of *Tp2* mRNA (8.1 h in WT vs 4.5 h in KI), *Prm2* mRNA (15 h in WT vs 3.2 h in KI) and *Tssk6* mRNA (9.2 h in WT vs 3 h in KI) were significantly reduced in GRTH-KI$^{h/h}$ mice compared to WT mice (Fig. 8C). This suggests that phospho-GRTH associates with *Tp2*, *Prm2 and Tssk6* mRNAs at cytoplasmic sites and presumably protect them from degradation. Consequently its absence causes the total loss of their protein expression in GRTH-KI$^{h/h}$ mice testis.

Discussion

This study has demonstrated that the GRTH-KI homozygous mice with $R^{242}H$ mutation lack the cytoplasmic phospho-form of GRTH while maintaining nuclear non-phospho species. These mice are sterile and lack sperm due to failure of round

spermatid to elongate while displayed normal mating behavior and basal circulating testosterone levels within the normal range. Phospho-GRTH was found to prevent testicular germ cell apoptosis and to be involved in maintaining the structure of the CB in RS. These are dense formations in the cytoplasm and a site for storage and/or degradation of mRNAs. TP2 and PRM2 protein expression was completely abolished in GRTH-KI mice and significant reductions of mRNA expression were observed in total and cytoplasmic mRNAs indicating a requisite role of phospho-GRTH in gene expression. Phospho-GRTH associates with relevant messages at cytoplasmic sites presumably for transport to the CB for storage prior to translation at precise stages of spermatogenesis and as a participant of the translational process in WT mice. We linked the lack of cytoplasmic phospho-GRTH in the GRTH-KI mice, to the increased mRNA degradation observed as revealed by the major decrease in their half-lives in GRTH-KI mice.

The absence of the phospho-form of GRTH in the GRTH-KI mice resemble our findings in COS-1 cells transfected the mutant $R^{242}H$ GRTH found in patients (14). We have previously determined that PKA is the kinase responsible for GRTH phosphorylation at Thr residue(s) (6). The 61 kDa phospho form of GRTH observed in cytosolic fractions of COS-1 cells transfected with the pCMV-GRTH-WT construct was highly induced by cyclic AMP. Three putative PKA phospho-sites at Thr 212, 239 and 408 were predicted by scanning analysis. Changes in basicity caused by the mutation $R^{242}H$ could result in a conformational change and consequently prevent the phosphorylation at an adjacent threonine in the GRTH molecule (14).

The 61 kDa phospho-GRTH which is solely found in the cytoplasm of germ cells and in association with the CB of RS in the WT mice (6), was absent in GRTH-KI mice as demonstrated by western blot analysis and immnunofluorescence studies (Fig. 1E). In contrast, the nuclear non-phospho form was unchanged. In addition, there was a significant decrease in the size of the CB revealed by electron microscopy (EM) studies indicating the relevance of phospho-GRTH in the structure of this specific germ cell cytoplasmic body. Moreover, it indicates that the identical changes in CB previously observed in KO mice resulted primarily from the lack of phospho-GRTH. These non-membrane cytoplasmic structures found in the vicinity of the nucleus of RS are repository of mRNAs presumably as mRNPs relevant to spermatogenesis awaiting for translation. At this site also mRNAs are likely to undergo repression and/or degradation. The CB resemble somatic P-bodies which are viewed as dynamic reservoirs of untranslated mRNA (19). As in the KO mice, major apoptosis was observed in RS and found also to a lesser degree in pachytene SP (5). In contrast, no changes in miRNAs were found in the KI versus the major increases observed in KO mice. This is consistent with their connection to the nuclear form (non-phospho GRTH) which in the WT was proposed to down-regulate the expression of members of the microprocessor complex (Drosha and DGCR8) at the transcriptional level with consequent reduction of relevant Pri-miRNAs (18, Table 1).

During the process of spermiogenesis where round spermatid undergo elongation, histones are first replaced by transition proteins (TP1 and TP2) and subsequently by protamines (PRM1/PRM2). These are highly basic proteins that facilitate hyper-chromatin condensation and reshaping the nucleus of round spermatid (20). In *Prm2*-deficient mice, DNA-hypercondensation and acrosome formation was drastically impaired (21). GRTH-KI mice showed abnormal acrosome formation in RS. There are other participant factors in this development including TSSK6, HSP90 and Histone variant H2AX. All these have an essential role in chromatin condensation and reshaping of spermatids (16). TSSK6 is expressed in ES, and is absent in the GRTH-KI mice due to arrest at round spermatid stage 8 just prior to elongation. The heat shock protein 90 chaperone, which is expressed in round and ES interacts with TSSK6 and facilitates the phosphorylation of histone variant H2AX (16). Tssk6 null mice revealed DNA condensation defects and sperm with abnormal morphology and reduced motility (22). The complete loss of chromatin remodeling gene expression (TP2 and PRM2) and TSSK6 in GRTH-KI mice could contribute to the arrest of spemiogenesis where RS fail to elongate. Phospho-GRTH plays an important role in storage of germ cell specific mRNAs which are transported by non-phospho GRTH from nucleus to the cytoplasm. In cytoplasm, phospho-GRTH may participate in their subsequent transport to the CB in RS and presumably in subsequent translation at later stages of spermatogenesis (3, 4, 11 and this study). The reduced size of CB found in RS of GRTH-KI mice with spermatogenic arrest indicates an essential requirement of phospho-GRTH to maintain the structural integrity of the CB for subsequent translation of relevant genes (like *Tssk6*, *Tp1, Tp2* and *Prm2 and others*). The lack of expression of these chromatin remodelers in GRTH-KI mice is may be due to their mRNAs failure to undergo translational process. In KI mice, Tp2 and presumably Tp1 found in RS showed significant reduction of their mRNAs that eventually undergo degradation as evident by decrease in their mRNA half-lives when compared to WT. In the case of PRMs and TSSK6 protein expression in ES, the marked reduction of mRNAs in RS and their failure of storage in the CB are most likely the cause of their lack of expression.

We have shown that phospho-GRTH has an important role in translation of *Tp2* in a 3′-UTRs dependent manner. In eukaryotes, several reports indicate translational control mediated by the 3′-UTRs of mRNAs. 3′-UTRs of mRNA contain cis-acting regulatory elements bound by RNA binding proteins (RBPs) that govern the regulation of protein translation (23). RBPs function in concert with different types of factors that are recruited to 3′-UTRs of genes which can behave as a repressor or activator of translation depending on the interacting co-factors or on post-translational modifications (24). In the case of Drosophila, Bruno factor binding to the 3′-UTR of oskar mRNA and Xenopus cytoplasmic polyadenylation element-binding protein (CPEB) binding to the 3′-UTR of cyclin B1 mRNA, eIF4E (DEAD-box RNA helicase) is recruited to repress the translation (25,26). In contrast, during

Table 1. Comparative parameters in germ cells of GRTH-KO and GRTH-KI mice

	GRTH-KO	GRTH-KI
Non-phospho-GRTH (Nuclear)	No	Yes
Non-phospho-GRTH (cytoplasm)	No	Yes
Phospho-GRTH (cytoplasm)	No	No
mRNA Nuclear Transport	No	Yes
Chromatoid Body (size)	↓	↓
Apoptosis	↑	↑
miRNAs	↑	NC
TP2 & Prm2 proteins	No	No

No = not present; Yes = present; NC = no change; Heterozygous not different from WT.

oocyte maturation in Xenopus, phosphorylation of CPEB promotes its interaction with the cleavage and polyadenylation specificity factor and the poly(A) polymerase GLD-2, which elongates the poly(A) tail leading to increased translation (23,26). Studies using transgenic mice show that the 3′ UTR of *Prm1/2* and *Tp2* is responsible for correct temporal translation of their mRNAs during spermatogenesis (27,28). Premature translation of *Tp2* mRNA causes sperm abnormalities and consequently, male infertility (29). These previous studies using TP2 transgenic mice supports the finding that GRTH promotes translational expression of *Tp2* mRNA in a 3′UTR dependent manner.

Taken together our findings demonstrate that the loss of phospho-GRTH in KI mice has a profund effects on the mRNA levels, their accumulation in the CB, the protein expression of chromatin remodelling genes, *Tp2, Prm2* and *Tssk6* and the elongation process of RS during spermiogenesis. Also, we can conclude that the heterozygous mutation $R^{242}H$ observed in the patients was not the cause of their azoospermia (14) since in the KI (this study) and KO models (5) only homozygous mice were infertile. A very recent study from our laboratory has demonstrated that Thr 239 is the site of phosphorylation of GRTH by cAMP dependent PKA (30). This site was found to be structurally adjacent to the $R^{242}H$ mutant found in patients which abolished the phosphorylation of GRTH (14). The various functions of GRTH/DDX25 provide a fertile ground for the development of a male contraceptive. Studies based on the abolition of pGRTH by mimicking the structural impact of the mutation observed in patients provide the framework for drug design of a reversible inhibitor for use as male contraceptive.

Materials and Methods

Generation of GRTH-KI targeting vector and genotyping

Mouse genomic BAC clone containing the 20Kb GRTH gene was used to construct the targeting vector. The targeting vector [mgrth5′-EGFP-loxP-T2A-hGRTHcDNA-SV40pA-loxP-Frt-Neo-Frt-loxP-mgrth3′-DT-A] contains 5 kb fragment of mice GRTH 5′-flanking region (5′end homologous arm), exon 1 of the mice GRTH gene, followed by a EGFP reporter sequence, loxP site, 2A self-cleaving peptide sequence, cDNA sequence from the human GRTH gene with $R^{242}H$ mutation, a human SV40 sequence, a loxP site and a PGK-Neo cassette flanked by two flippase recognition target (FRT) sites, a loxP site, a 3.0 kb fragment of the GRTH gene from intron 5 to intron 7 (3′ end homologous arm), and a diphtheria toxin A (DT-A) fragment gene (Fig. 1A). The region containing the $R^{242}H$ mutation is 100% identical in human and mouse. The targeting vector was transfected into 129/SVJ mice ES cells by electroporation and screened for positive ES clones that has integrated the construct by homologous recombination by PCR and confirmed by Southern blotting (data not shown). The targeted ES cells were microinjected into C57BL/6 recipient blastocysts to obtain chimeras in Transgenic Core Facility of National Institute Mental Health, NIH. The chimeric male mice were crossed with female C57BL/6 mice to generate heterozygotes carrying the recombinant allele. These mice then crossed with *FLP* deleter transgenic mice (Jackson Laboratory, MA) to eliminate the FRT flanked neomycin cassette. Genotyping of the mice was performed by PCR using two set of primers Geno F1/Geno R1 and Geno F2/Geno R2 (Table 2) to detect targeted GRTH allele and mice GRTH allele, respectively.

Table 2. List of Primers used for genotyping and real-time PCR analysis

Primer Name	Primer Sequence 5′—3′
Geno F1	AGAACGGCATCAAGGTGAAC
Geno R1	GCCTCCCCACAGTAACGAC
Geno F2	GATACCTAAGTTGGCTAGGTATCCTGAG
Geno R2	ATAGTTGCCCAAGCTGCTACCCCAGTTCCA
GRTH F	CAGATTATAATTGGCACTCCTG
GRTH R	CATTCGGAGGGTAGAGCTCT
TP2 F	GCTCTAGCTCCAGCCCCAGC
TP2 R	CTTGTATCTTCGCCCTGAG
PRM2 F	GGCAAGGGCTGAGCCCAGAGC
PRM2 R	TCGGGATCTTCTGCAGCCTCTGC
TSSK6 F	CCGCGAAGTCGCCGCGCGCCACTG
TSSK6 R	TCTCTCTTCTCTTTGCGCCCCTCC
HMG2 F	GCGAAGAAACTGGGTGAGATGTG
HMG2 R	CCTCATCTTCTGGTTCGTTCTTC
tACE F	ATGGGCCACATCCAGTATTTCATGCA
tACE R	GATCTTGTCGAGGGCCATCTTCATTAG
β-actin F	AGGCATTGCTGACAGGATGCAG
β-actin R	AGCACTTGCGGTGCACGATG
miR-34c RT	GTCGTATCCAGTGCAGGGTCCGAGGTATTCGCACTGGATACGACGCAATC
miR-34c F	GCAGCCAGGCAGTGTAGTTAGC
miR-469 RT	GTCGTATCCAGTGCAGGGTCCGAGGTATTCGCACTGGATACGACGGACAC
miR-469 F	GCTTCCTGCCTCTTTCATTGATC
miR let-7e RT	GTCGTATCCAGTGCAGGGTCCGAGGTATTCGCACTGGATACGACAACCAT
miR let-7e F	GCCGCCAGAGGTAGTAGGTTG
miR Universal R	AGTGCAGGGTCCGAGG
U6 RT	CGCTTCACGAATTTGCGTGTC
U6 F	TCGCTTCGGCAGCACATATAC
U6 R	GCGTGTCATCCTTGCGCAG

Animals were housed in pathogen-free, temperature- and light-controlled conditions (22°C), with an alternating light–dark cycle with 14 h of light and 10 h of darkness. All studies were approved by National Institute of Child Health and Human Development Animal Care and Use Committee.

Histology

Histological studies were performed to monitor morphological changes in seminiferous tubules of WT and GRTH-KI mice testis. Adult mice testes and epididymes were fixed in 4% paraformaldehyde and embedded in paraffin. Serial sections were subjected to Hematoxylin & Eosin staining and examined under Ziess AxioSkope brightfield microscope. In parallel studies, PAS staining was used to stain acrosomes to determine the spermatogenic stage of seminiferous tubules.

Serum testosterone measurement

Serum testosterone levels of WT and GRTH-KI mice were measured using a chemiluminescence immunoassay kit (DRG International, NJ), with a sensitivity of 0.05 ng/ml, according to the manufacturer's protocol.

EM analysis

Small fragments of testicular tissue from WT and GRTH-KI mice were fixed in 2.5% glutaraldehyde buffer at 4°C for 18 h, post-fixed in 1% osmium tetroxide, and en bloc-stained with 2% uranyl acetate, dehydrated and embedded in Spurr's epoxy. Ultra thin sections were made using Leica EM ultramicrotome and post-stained with lead citrate and later observed under a transmission EM.

Western blot analysis

Total protein extracts from testis tissues were prepared using RIPA lysis buffer (Upstate, Temecula, CA) containing protease and phosphatase inhibitor cocktail (Roche Applied Sciences, CA). Cytoplasmic and nuclear protein extracts of testis tissue were prepared using NE-*PER Nuclear* and *Cytoplasmic Extraction Kit* (ThermoScientific, MA) containing protease and phosphatase inhibitor cocktail. The protein lysates were centrifuged at 1500 g for 10 min. The supernatant was collected and protein concentration was determined by the Bradford assay (Bio-rad Laboratories, CA). The protein extracts (75 µg) were separated using 4–12% Bis-Tris gel (Invitrogen) and transferred onto nitrocellulose membrane. The membrane was blocked with 5% skimmed milk powder in phosphate buffer saline and then incubated either with affinity-purified anti-GRTH rabbit polyclonal antibody at 1:500 dilution (6) or β-actin (Santa Cruz, CA; sc69879) antibody at 1:2000 dilution. After the incubation of primary antibody and washing steps, the membranes were incubated with the respective secondary antibodies conjugated with HRP at 1:2000 dilution. Immunosignals were detected by a super-signal chemiluminescence system (Pierce Biotechnology, MA).

Immunofluorescence

For immunofluorescence studies, germ cell preparations were obtained by squeezing the seminiferous tubules with fine forceps in 100 µl of 100 mM sucrose solution on petri dish. The germ cell suspensions were spread on slides pre-coated with 1% paraformaldehyde solution with 0.15% Triton X-100 and dried overnight in a humidified box. The fixed cells were permeabilized with 0.2% Triton X-100 for 5 min and blocked in 5% BSA for 1 h at room temperature. The slides were incubated with specific GRTH polyclonal antibody (1:250 dilution) at 4°C, overnight. Slides were subsequently incubated with Alexa Fluor 568 for 1 h at room temperature. ProLong Gold antifade reagent with nuclei stain 4',6-diamidino-2-phenylindole (Invitrogen, CA) was used to mount the slides. These slides were visualized using an Ziess Axioplan 2 imaging fluorescence microscope and images were taken using an AxioCam with Axiovision v4.5 software (Carl Zeiss, CA). To localize apoptotic germs cells in seminiferous tubules, TUNEL IHC assay was carried out in testicular sections using TACS2 TdT DAB *in situ* labeling kit (Trevigen, MD).

Immunoprecipitation and RT-PCR Analysis

Cytoplasmic and nuclear extracts (0.5 mg) isolated from WT and GRTH-KI$^{h/h}$ mice using a NE-*PER Nuclear* and *Cytoplasmic Extraction Kit* (ThermoScientific, MA) were initially subjected to preclearing by incubation with 50 µl of protein A-agarose beads and 1 µg of rabbit IgG in Immunoprecipitation (IP) binding buffer (ThermoScientific, MA) with gentle agitation for 30 min at 4°C. Then the supernatant was incubated with 4 µg affinity-purified anti-GRTH rabbit polyclonal antibody for overnight at 4°C to co-immunoprecipitate the GRTH-ribonucleoprotein complex. A total of 50 µl of protein A-agarose beads was added and incubated for 2 h at 4°C. The GRTH-ribonucleoprotein complex bound to protein A-agarose was washed three times with IP binding buffer. The RNA from this GRTH-ribonucleoprotein complexes was isolated by phenol/chloroform/isoamyl alcohol (25:24:1, v/v; Invitrogen). First-strand cDNA was prepared using a SuperScript III first-strand synthesis kit (ThermoScientific, MA) and real-time PCR was performed with Fast SYBR green using specific set of primers for Tp2, Prm2 and GRTH (Table 2) in a 7500 Fast Real-Time PCR machine (Applied Biosystems, CA).

Luciferase assay

COS-1 cells (0.1×10^6 cells/well) were seeded in 12 well plate 24 h before transfection. Cells were transfected with psiCHECK-2 construct alone carrying the TP2 coding region along with 3′ UTR (15) or co-transfection with either pCMV-GRTH-WT construct (expression WT human GRTH protein) or pCMV-GRTH-Mut ($R^{242}H$) construct (expression WT human GRTH protein with a mutation at 242 amino acid from R to H). To induce the phosphorylation of GRTH, cells were also co-tranfected with plamid expressing PKA catalytic subunit α. After 48 h of transfection cells were lysed with passive lysis buffer (Promega, WI). Firefly and *Renilla* luciferase activities were measured with the dual-luciferase reporter system (Promega) using a Tristar luminometer (Berthold Technologies, TN).

microRNA analysis

To assess the expression of testis specific miRNA's (miR469, miR34c), and Let7e quantitative real time RT-PCR analysis was carried as previously described (15). Total RNA enriched for small RNAs was prepared from testis of WT or GRTH-KI mice using miRNeasy mini kit (Qiagen). 500 ng of total RNA was reversed

transcribed with miRNA specific RT primers (Table 2) using TaqMan microRNA reverse transcription kit (Applied Biosystems) according to the manufacturer's protocol. The expression levels were measured in triplicate using SYBR Green PCR Master Mix (Applied Biosystems) with miRNA-specific forward primers and a universal reverse primer (Table 2) on an ABI 7500 FAST real time PCR system (Applied Biosystems) with the following conditions: 95°C for 20 s followed by 40 cycles of 95°C for 3 s and 60°C for 30s. The miRNA expression levels were normalized to U6 small nuclear RNA, and fold-change was determined by the $2^{-\Delta\Delta Ct}$ method.

mRNA stability assay

Seminiferous tubules cultures from WT and GRTH-KI mice were prepared as described previously (7). Briefly, testes were excised, decapsulated and treated with collagenase to isolate the seminiferous tubules which where then cut into small segments and incubated in Medium 199 containing 0.1% BSA for 1 h, followed by incubation with 20 µg/ml actinomycin D for 24 h at five different time points. Total RNA was isolated from different time point samples, cDNA was prepared, and *Tp2, Prm2* and *Tssk6* mRNAs levels were quantitated by real-time PCR as described above.

Statistical analysis

The significance of the differences between groups was determined by Tukey's multiple-comparison test (one-way ANOVA analysis) using the Prism software program (GraphPad Software, Inc, San Diego, CA).

Acknowledgements

We thank Mr Daniel Abebe for his expert assistance with the animal work and Dr Louis Dye for EM studies.

Conflict of Interest statement. None declared.

Funding

This work was supported by the National Institutes of Health Intramural Research Program through the *Eunice Kennedy Shriver* National Institute of Child Health and Human Development.

References

1. Tang, P.Z., Tsai-Morris, C.H. and Dufau, M.L. (1999) A novel gonadotropin-regulated testicular RNA helicase. A new member of the dead-box family. *J. Biol.Chem.*, **274**, 37932–37940.
2. Sheng, Y., Tsai-Morris, C.H. and Dufau, M.L. (2003) Cell-specific and hormone-regulated expression of gonadotropin-regulated testicular RNA helicase gene (GRTH/Ddx25) resulting from alternative utilization of translation initiation codons in the rat testis. *J. Biol. Chem.*, **278**, 27796–27803.
3. Dufau, M.L. and Tsai-Morris, C.H. (2007) Gonadotropin-regulated testicular helicase (GRTH/DDX25): an essential regulator of spermatogenesis. *Trends Endocrinol. Metab.*, **18**, 314–320.
4. Tsai-Morris, C.H., Sheng, Y., Gutti, R.K., Tang, P.Z. and Dufau, M.L. (2010) Gonadotropin-regulated testicular RNA helicase (GRTH/DDX25): a multifunctional protein essential for spermatogenesis. *J. Androl.*, **31**, 45–52.
5. Tsai-Morris, C.H., Sheng, Y., Lee, E., Lei, K.J. and Dufau, M.L. (2004) Gonadotropin-regulated testicular RNA helicase (GRTH/Ddx25) is essential for spermatid development and completion of spermatogenesis. *Proc. Natl. Acad. Sci. U. S. A.*, **101**, 6373–6378.
6. Sheng, Y., Tsai-Morris, C.H., Gutti, R., Maeda, Y. and Dufau, M.L. (2006) Gonadotropin-regulated testicular RNA helicase (GRTH/Ddx25) is a transport protein involved in gene-specific mRNA export and protein translation during spermatogenesis. *J. Biol. Chem.*, **281**, 35048–35056.
7. Sato, H., Tsai-Morris, C.H. and Dufau, M.L. (2010) Relevance of gonadotropin-regulated testicular RNA helicase (GRTH/DDX25) in the structural integrity of the chromatoid body during spermatogenesis. *Biochim. Biophys. Acta*, **1803**, 534–543.
8. Villar, J., Tsai-Morris, C.H., Dai, L. and Dufau, M.L. (2012) Androgen-induced activation of gonadotropin-regulated testicular RNA helicase (GRTH/Ddx25) transcription: essential role of a nonclassical androgen response element half-site. *Mol. Cell. Biol.*, **32**, 1566–1580.
9. Tsai-Morris, C.H., Sheng, Y., Gutti, R., Li, J., Pickel, J. and Dufau, M.L. (2010) Gonadotropin-regulated testicular RNA helicase (GRTH/DDX25) gene: cell-specific expression and transcriptional regulation by androgen in transgenic mouse testis. *J. Cell. Biochem.*, **109**, 1142–1147.
10. Kavarthapu, R., Tsai-Morris, C.H., Fukushima, M., Pickel, J. and Dufau, M.L. (2013) A 5′-flanking region of gonadotropin-regulated testicular RNA helicase (GRTH/DDX25) gene directs its cell-specific androgen regulated gene expression in testicular germ cells. *Endocrinology*, **154**, 2200–2207.
11. Kavarthapu, R. and Dufau, M.L. (2015) Germ cell nuclear factor (GCNF/RTR) regulates transcription of gonadotropin-regulated testicular RNA helicase (GRTH/DDX25) in testicular germ cells - the androgen connection. *Mol. Endocrinol.*, **29**, 1792–1804.
12. Fukushima, M., Villar, J., Tsai-Morris, C.H. and Dufau, M.L. (2011) Gonadotropin-regulated testicular RNA helicase (GRTH/DDX25), a negative regulator of luteinizing/chorionic gonadotropin hormone-induced steroidogenesis in Leydig cells: central role of steroidogenic acute regulatory protein (StAR). *J. Biol. Chem.*, **286**, 29932–29940.
13. Tsai-Morris, C.H., Lei, S., Jiang, Q., Sheng, Y. and Dufau, M.L. (2004) Genomic organization and transcriptional analysis of gonadotropin-regulated testicular RNA helicase-GRTH/DDX25 gene. *Gene*, **331**, 83–94.
14. Tsai-Morris, C.H., Koh, E., Sheng, Y., Maeda, Y., Gutti, R., Namiki, M. and Dufau, M.L. (2007) Polymorphism of the GRTH/DDX25 gene in normal and infertile Japanese men: a missense mutation associated with loss of GRTH phosphorylation. *Mol. Hum. Reprod.*, **13**, 887–892.
15. Tsai-Morris, C.H., Sato, H., Gutti, R. and Dufau, M.L. (2012) Role of gonadotropin regulated testicular RNA helicase (GRTH/Ddx25) on polysomal associated mRNAs in mouse testis. *PLoS One*, **7**, 10.1371/journal.pone.0032470.
16. Jha, K.N., Tripurani, S.K. and Johnson, G.R. (2017) TSSK6 is required for γH2AX formation and the histone-to-protamine transition during spermiogenesis. *J. Cell. Sci.*, **130**, 1835–1844.
17. Dai, L., Tsai-Morris, C.H., Sato, H., Villar, J., Kang, J.H., Zhang, J. and Dufau, M.L. (2011) Testis-specific miRNA-469 up-regulated in gonadotropin-regulated testicular RNA helicase (GRTH/DDX25)-null mice silences transition protein 2 and

protamine 2 messages at sites within coding region: implications of its role in germ cell development. *J. Biol. Chem.*, **286**, 44306–44318.
18. Yang, R., Tsai-Morris, C.H., Kang, J.H. and Dufau, M.L. (2015) Elucidation of RNA binding regions of gonadotropin-regulated testicular RNA helicase (GRTH/DDX25) to transcripts of a chromatin remodeling protein essential for spermatogenesis. *Horm. Mol. Biol. Clin. Investig.*, **22**, 119–130.
19. Franks, T.M. and Lykke-Andersen, J. (2008) The control of mRNA decapping and P-body formation. *Mol. Cell.*, **32**, 605–615.
20. Schneider, S., Balbach, M., Jikeli, J.F., Fietz, D., Nettersheim, D., Jostes, S., Schmidt, R., Kressin, M., Bergmann, M., Wachten, D. *et al.* (2016) Re-visiting the Protamine-2 locus: deletion, but not haploinsufficiency, renders male mice infertile. *Sci. Rep.*, **6**, 10.1038/srep36764.
21. Boa, J. and Bedfors, M.T. (2016) Epigenetic regulation of the histone-to-protamine transition during spermiogenesis. *Reproduction*, **151**, 55–70.
22. Sosnik, J., Miranda, P.V., Spiridonov, N.A., Yoon, S.Y., Fissore, R.A., Johnson, G.R. and Visconti, P.E. (2009) Tssk6 is required for Izumo relocalization and gamete fusion in the mouse. *J. Cell. Sci.*, **122**, 2741–2749.
23. Kuersten, S. and Goodwin, E.B. (2003) The power of the 3' UTR: translational control and development. *Nat. Rev. Genet.*, **4**, 626–637.
24. Szostak, E. and Gebauer, F. (2013) Translational control by 3'-UTR-binding proteins. *Brief. Funct. Genomics*, **12**, 58–65.
25. Nakamura, A., Sato, K. and Hanyu-Nakamura, K. (2004) Drosophila cup is an eIF4E binding protein that associates with Bruno and regulates oskar mRNA translation in oogenesis. *Dev. Cell.*, **6**, 69–78.
26. Stebbins-Boaz, B., Cao, Q., de Moor, C.H., Mendez, R. and Richter, J.D. (1999) Maskin is a CPEB-associated factor that transiently interacts with elF-4 E. *Mol. Cell.*, **4**, 1017–1027.
27. Villalba, A., Coll, O. and Gebauer, F. (2011) Cytoplasmic polyadenylation and translational control. *Curr. Opin. Genet. Dev.*, **21**, 452–457.
28. Schäfer, M., Nayernia, K., Engel, W. and Schäfer, U. (1995) Translational control in spermatogenesis. *Dev. Biol.*, **172**, 344–352.
29. Tseden, K., Topaloglu, O., Meinhardt, A., Dev, A., Adham, I., Müller, C., Wolf, S., Böhm, D., Schlüter, G., Engel, W. *et al.* (2007) Premature translation of transition protein 2 mRNA causes sperm abnormalities and male infertility. *Mol. Reprod. Dev.*, **74**, 273–279.
30. Raju, M., Hassan, S.H., Kavarthapu, R., Anbazhagan, R., Dufau, M.L. (2019) Characterization of the phosphorylation site of GRTH/DDX25 and protein kinase a binding interface provides structural basis for the design of a non-hormonal male contraceptive. *Sci. Rep.*, doi: 10.1038/s41598-019-42857-9.